Gamma decays of the first $T = 3/2$ states in ^{9}Be and ^{9}B†

P. A. Dickey, P. L. Dyer,* K. A. Snover, and E. G. Adelberger
Nuclear Physics Laboratory, University of Washington, Seattle, Washington 98195
(Received 8 May 1978)

We have measured the γ-ray branching ratios of the lowest $T = 3/2$ states in the isospin mirror nuclei ^{9}Be and ^{9}B. The ratio of reduced $M1$ transition strengths $B_{\gamma_2}(M1)/B_{\gamma_0}(M1) = 1.97 \pm 0.12$ in ^{9}Be and 1.76 ± 0.21 in ^{9}Be and hence shows no charge asymmetry, in agreement with the usual selection rules for $\Delta T = 1$ electromagnetic transitions. A value of $(1.9 \pm 2.1)\%$ is derived for the relative size of any isotensor amplitudes for the $M1$ transitions. For the total widths of the $T = 3/2$ levels we find $\Gamma(^9\text{Be}) = 381 \pm 33$ eV, $\Gamma(^9\text{B}) = 395 \pm 42$ eV, and $\Gamma(^9\text{B})/\Gamma(^9\text{Be}) = 1.04 \pm 0.10$, assuming $B_{\gamma_0}(M1,^9\text{B}) = B_{\gamma_0}(M1,^9\text{Be})$ and $\Gamma_{\gamma_0} = 6.9 \pm 0.5$ eV in ^{9}Be. The γ-ray transition strengths are compared with theoretical calculations and with the analogous β decay of ^{9}Li.

[NUCLEAR REACTIONS ^{7}Li(^{3}He,$p\gamma$), ^{7}Li(He,$n\gamma$), particle-γ coincidence; measured Γ_{γ_i}/Γ and deduced Γ_{γ_i} and Γ for ^{9}Be($T=\frac{3}{2}$) and ^{9}B($T=\frac{3}{2}$); symmetry of mirror transitions.]

I. INTRODUCTION

The isospin mirror γ decays of the lowest $T=\frac{3}{2}$ levels in $A=4N+1$ nuclei provide tests of both the isospin purity of the nuclear states and the isospin character of the electromagnetic interaction. Isovector γ transitions in mirror nuclei are expected to have identical strengths[1] if the nuclear states are charge symmetric and if only isoscalar and isovector components are present in the electromagnetic current. An asymmetry in the rates for analogous isovector γ transitions must be related either to the presence of an isotensor electromagnetic current in nuclei or to a failure of strict charge symmetry in the nuclear states.

Recently a precise comparison[2] of the isovector γ decay widths of the lowest $T=\frac{3}{2}$ levels in ^{13}C and ^{13}N showed no asymmetry at the 13% level in the mirror $M1$ decays γ_0 and γ_2. These decays are particularly suitable as a test for isotensor currents because they are relatively insensitive to nuclear structure since the transitions are strong and the $M1$ operator has no radial dependence in the long wavelength limit. Upper limits of 2–7% deduced for the ratio of isotensor to isoscalar amplitudes in mass 13 represent an improvement over an earlier 10% upper limit by Blin-Stoyle,[3] but are still considerably larger than theoretical expectations.[4] To date no experimental limit of comparable stringency has been available for mass 9.

The γ decay branching ratios can also be used to infer the total widths of the $T=\frac{3}{2}$ levels. The total widths, which arise from isospin-forbidden particle decays, measure the $T=\frac{1}{2}$ admixtures in the $T=\frac{3}{2}$ levels. Even if the radiative widths Γ_{γ_0} are not known for both nuclei, the expectation that asymmetries in the $M1$ decays will be quite small justifies the assumption that for this purpose the reduced ground state decay widths may be taken to be equal. Then the total widths can be deduced from the branching ratios Γ_{γ_0}/Γ, which can be measured quite accurately. In each of the mass 13 (Ref. 2), 17 (Ref. 5), and 21 (Ref. 6) systems the $T_z=\frac{1}{2}$, $T=\frac{3}{2}$ level is much broader than the $T_z=-\frac{1}{2}$ level. The same is true in mass 25 when reduced nucleon decay widths are compared.[7,8] On the other hand, the mirror levels are already known to be of comparable width in mass 9 ($\Gamma_{^9\text{Be}}/\Gamma_{^9\text{B}} = 1.2 \pm 0.5$).[9] Our measurement of the branching ratios in mass 9 substantially reduces the uncertainty in the ratio of the total widths in this unusual case, which should serve as an important test for models of isospin mixing in $T=\frac{3}{2}$ levels.

In this paper we report a measurement of the γ decays of the lowest $T=\frac{3}{2}$ levels in mass 9 with precision comparable to that reported for mass 13. Absolute branching ratios have been obtained in both ^{9}Be and ^{9}B permitting a comparison of the total widths of the $T=\frac{3}{2}$ levels with 10% uncertainty. The mass 9 isovector γ decays have been studied previously by Adloff *et al.*,[10] but absolute branching ratios were measured only for ^{9}Be and the poor γ-ray energy resolution of that experiment resulted in large uncertainties and a mistaken assignment of an excited-state branch.

II. EXPERIMENT

The mirror reactions ^{7}Li(^{3}He,p)^{9}Be* and ^{7}Li(^{3}He,n)^{9}B* were used to populate the $T=\frac{3}{2}$ lev-

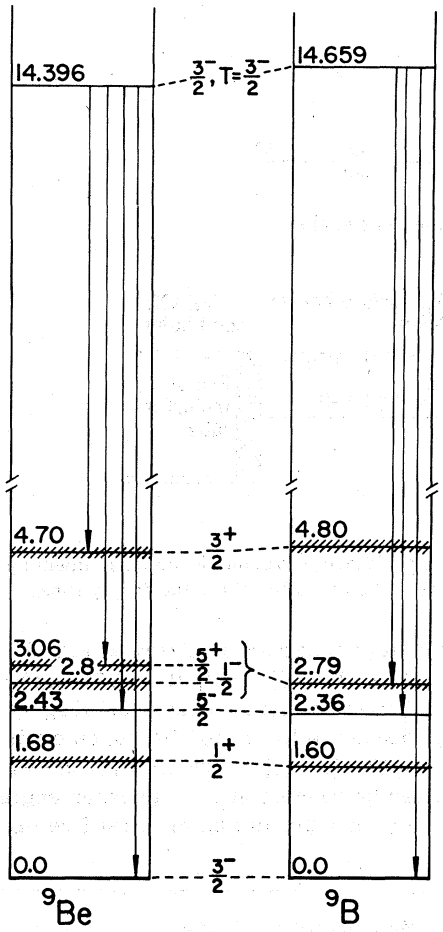

FIG. 1. Partial level schemes of the mass 9 mirror nuclei showing the γ decays of the $T=\frac{3}{2}$ levels whose branching ratios have been measured in this experiment.

els, and deexcitation γ rays were detected in coincidence with protons and neutrons. The γ decays of interest are indicated in Fig. 1. Absolute γ decay branching ratios were deduced from the $T=\frac{3}{2}$ particle group yield in singles and coincidence spectra. The experimental arrangement is illustrated in Fig. 2. Particles were detected at 0° to align the spin $\frac{3}{2}$ residual nuclei so that the total γ-ray yield could be inferred directly from a single measurement at $\theta_\gamma = 125°$, a zero of $P_2(\cos\theta_\gamma)$. γ rays were detected with 4% energy resolution in the University of Washington 25.4 cm $\times$ 25.4 cm NaI spectrometer. This spectrometer has an anticoincidence shield whose output was used to route the γ-ray pulses into "accept" and "reject" spectra of which only the accept spectrum was used for analysis. The proton detector was a ΔE-E telescope consisting of a 200 μm fully depleted Si surface barrier detector and a 3 mm Si(Li) detector. Neutrons were detected with either a 11.4 cm diam. $\times$ 2.5 cm or 12.7 cm diam. $\times$ 5.1 cm NE102 plastic scintillator viewed by an RCA 4522 photomultiplier.

Targets of approximately 200 μg/cm^2 of 99.9% enriched ^{7}Li metal were evaporated onto 200 μg/cm^2 Ni and 3 mg/cm^2 Ta backings and transferred in vacuum to the scattering chamber. Bombarding energies were carefully chosen to avoid ambiguities between γ rays from the decay of interest and coincidences arising from γ decays in the mirror nucleus which feed particle unstable levels.

A. $T = 3/2$ decays in ^{9}Be

A 7.5 MeV, 150 nA beam of ^{3}He^{++} ions from the University of Washington FN tandem accelerator bombarded the Ni backed target and was stopped in a 0.025 mm Ni foil placed in front of the proton detector. Protons populating the 14.396 MeV, $T=\frac{3}{2}$ state had a laboratory energy of about 1.2 MeV after passing through the foil. Three parameter [E_p, E_γ, and time-to-amplitude converter (TAC)] coincidence data were event recorded on magnetic tape; proton singles and coincidences were accumulated simultaneously through the same analog-to-digital converter (ADC).

The data tapes were played back with software windows on the TAC and γ ray spectra to locate the $T=\frac{3}{2}$ group in the particle spectrum. Figure 3 shows the particle singles and coincidence spectra in the vicinity of the $T=\frac{3}{2}$ group. The yield in singles was obtained by fitting the spectrum with a peak shape taken channel by channel from the coincidence peak shape. The peak height and the parameters of a quadratic background were varied to minimize χ^2, and then the fitted area was calculated. The fit is shown as a solid curve in the upper portion of Fig. 3; the smooth curve drawn through the coincidence spectrum below is the line shape used in the fit. The statistical error in the singles yield was ±1.7%.

The γ-decay spectrum of the $T=\frac{3}{2}$ state in ^{9}Be, shown in the upper portion of Fig. 4, was obtained by replaying the (^{3}He, $p\gamma$) data tapes with windows on both the TAC and particle spectra. Random coincidences have been subtracted. Fits to the spectra (shown as solid lines) will be discussed in Sec. III A.

B. $T = 3/2$ decays in ^{9}B

For the ^{9}B portion of the coincidence experiment the proton telescope was replaced by the neutron detector with the 11.4 cm $\times$ 2.5 cm scintillator, but the γ detection system was untouched. A 13 MeV ^{3}He^{++} beam bombarded the Ta backed foil and was stopped in a Ta Faraday cup inside the scattering chamber. Neutron energies were de-

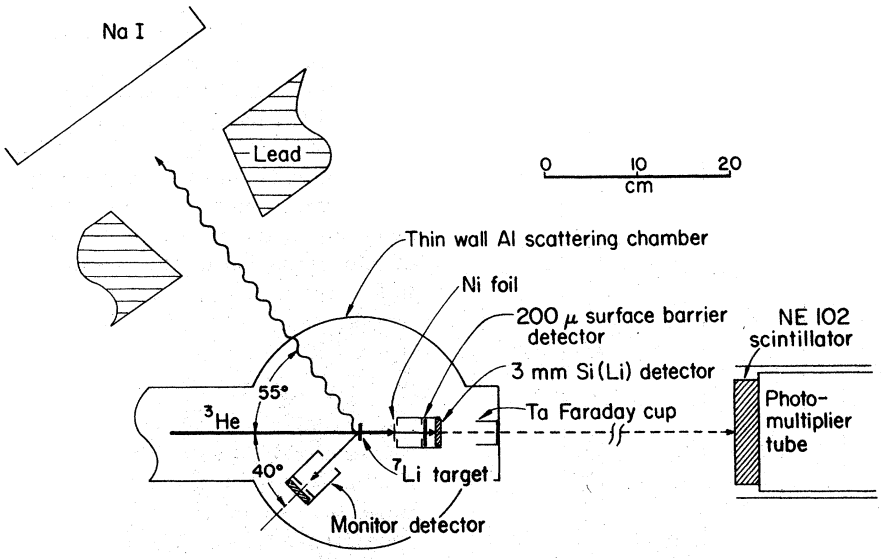

FIG. 2. Diagram of the experimental setup for the ^{7}Li(^{3}He,$p\gamma$)^{9}Be and ^{7}Li(^{3}He,$n\gamma$)^{9}B coincidence experiments and for the NaI efficiency measurement. The particle detector telescope was moved away from 0° for the (^{3}H,n) runs.

duced from time of flight (TOF) over a 60 cm path at 0°. The NaI detector provided the TOF start pulse in the coincidence experiment. A TOF spectrum is shown in Fig. 5 and the neutron detector energy spectrum is shown in Fig. 6. In addition to the ^{9}B($T=\frac{3}{2}$) level, the TOF spectrum shows a broad continuum consisting largely of neutron decays of low lying ^{9}Be states excited via ^{7}Li(^{3}He,p)^{9}Be*($T=\frac{3}{2}$)(γ). This continuum was minimized by running at a bombarding energy such that γ rays populating the first five excited

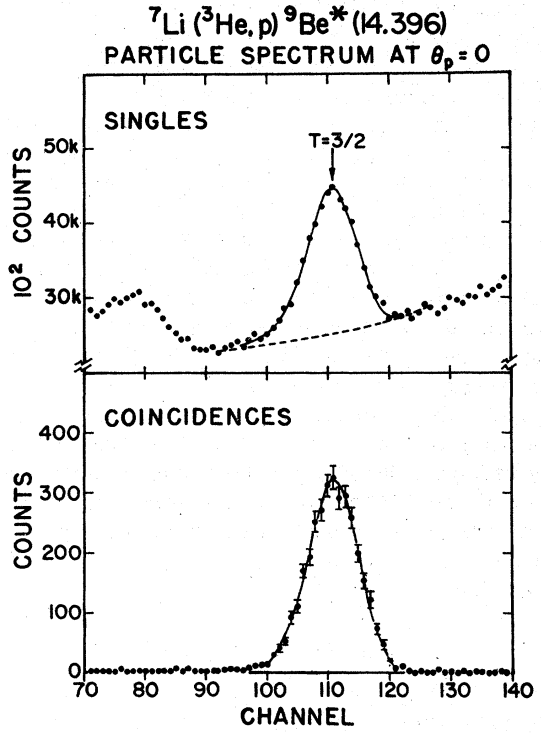

FIG. 3. Particle singles and coincidence spectra from ^{7}Li(^{3}He,$p\gamma$)^{9}Be at $E_{^3\mathrm{He}}=7.5$ MeV, $\theta_p=0°$. The spectra were accumulated through the same ADC. The smooth curve drawn through coincidence spectrum was used to fit the singles data.

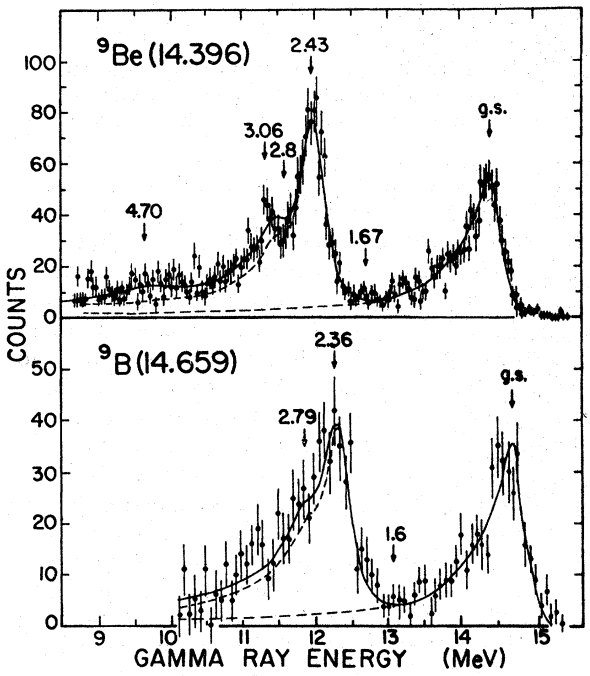

FIG. 4. Coincidence γ-ray spectra from the decay of $T=\frac{3}{2}$ levels in ^{9}Be (upper) and ^{9}B (lower). Solid curves are least squares fits discussed in the text.

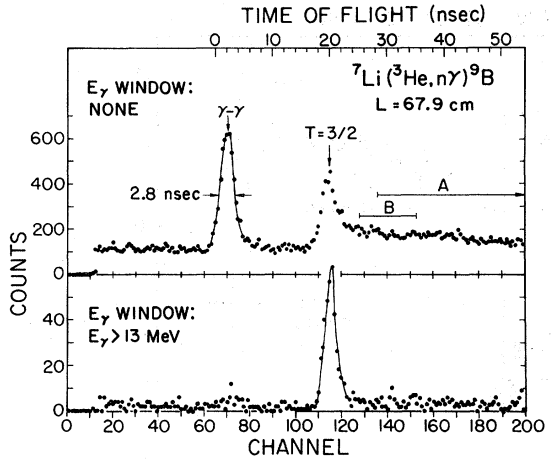

FIG. 5. Neutron time of flight spectra from the ^{7}Li(^{3}He,$n\gamma$)^{9}B coincidence experiment. The TAC is started by the NaI, stopped by the neutron detector. In the upper spectrum all NaI pulses are accepted; in the lower only pulses above 13 MeV are accepted. Region A is the kinematic locus for neutrons from the sequence ^{7}Li(^{3}He,$p\gamma$)^{9}Be(2.43)$\rightarrow 2\alpha+n$; region B is the locus for ^{7}Li(^{3}He,$p\gamma$)^{9}Be(2.8)(n)^{8}Be(g.s.).

states of ^{9}Be do not produce counts which lie underneath the $T=\frac{3}{2}$ neutron group.

A spectrum of γ rays from the decay of ^{9}B($T=\frac{3}{2}$) is shown in the lower part of Fig. 4. A small correction has been applied to this spectrum to subtract γ rays in coincidence with neutrons in the broad continuum. The correction was made by placing a series of contiguous narrow windows on the TOF spectrum in the continuum region (channels 125–180) and extrapolating the behavior of the coincident γ-ray spectrum to TOF channels 112–120 underlying the $T=\frac{3}{2}$ group. This correction makes a slight reduction in the 10 to 11.5 MeV portion of the γ-ray spectrum but has a

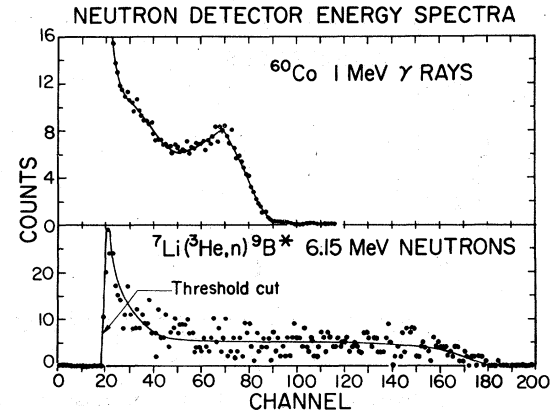

FIG. 6. Energy spectra in the neutron detector resulting from a ^{60}Co γ source (upper) and 6.15 MeV neutrons from ^{7}Li(^{3}He,$n\gamma$)^{9}B (lower).

negligible effect on the deduced branching ratios to the ground state or excited states up to 2.8 MeV.

The measurement of the ^{7}Li(^{3}He,n)^{9}B($T=\frac{3}{2}$) singles neutron yield, needed for the absolute branching ratios in ^{9}B, was performed at a later time with a pulsed ^{3}He beam, also at 13 MeV. The target for the singles measurement was 400 μg/cm^2 of ^{7}Li on 10 mg/cm^2 Ta. The neutron detector geometry differed from that used for the coincidence measurement because better resolution and hence a longer flight path was needed for the singles data. A 12.7 cm diam. $\times$ 5.1 cm thick NE102 scintillator was mounted on the photomultiplier and placed at 0°, 4.15 m from the target. Normalization of the coincidence and singles yields to each other was accomplished by measuring each relative to the ^{7}Li(^{3}He,p_0) yield in a monitor detector at $\theta=140°$.

The ratio of neutron detector efficiencies for the two geometries at a neutron energy of 6.15 MeV was calculated from the measured flight paths and scintillator dimensions. Since the ratio depends only weakly on the absolute intrinsic efficiency of the detector, the absolute intrinsic efficiency η_i was calculated using the formula[11]

$$\eta_i(E_n L)=\frac{E_n-B}{E_n}\,(1-e^{-n_H\sigma_H L}),$$

where n_H is the number of hydrogen atoms per cm^3, σ_H is the n-p scattering cross section, L is the scintillator thickness, and B is the discriminator bias. Christensen and Cocke[11] found this expression to agree to ±10% with their measured efficiency for 6 MeV neutrons in a detector similar to ours. The low energy discriminator threshold was carefully set for all runs at the peak in the spectrum of 60 keV γ rays from a ^{241}Am source ($B\approx 0.5$ MeV, but the ratio is independent of B). Using the values $n_H=0.0525\times10^{24}$ cm^{-3} and $\sigma_H=1.45\times10^{-24}$ cm^2 for NE102,[11] we obtain the ratio $\eta_i(L=5.08\text{ cm})/\eta_i(L=2.54\text{ cm})=1.83\pm0.02$. The error was estimated assuming an uncertainty of ±10% in $\eta_i(L=5.08$ cm) based on the experience of Christensen and Cocke. The ratio of efficiency-solid angle product for the coincidence and singles geometries was found to be

$$\frac{\eta_i\times\Omega\,(\text{coin.})}{\eta_i\times\Omega\,(\text{sing.})}=16.5\pm0.2\,.$$

The neutron TOF spectrum from the singles measurement is shown in Fig. 7. The TAC start pulse was derived from the neutron detector and the stop pulse from the beam buncher. The yield of the $T=\frac{3}{2}$ group was determined by subtracting a linear background under the peak. The statistical uncertainty in the peak area is ±4.7%; when the neutron detector efficiency and monitor cor-

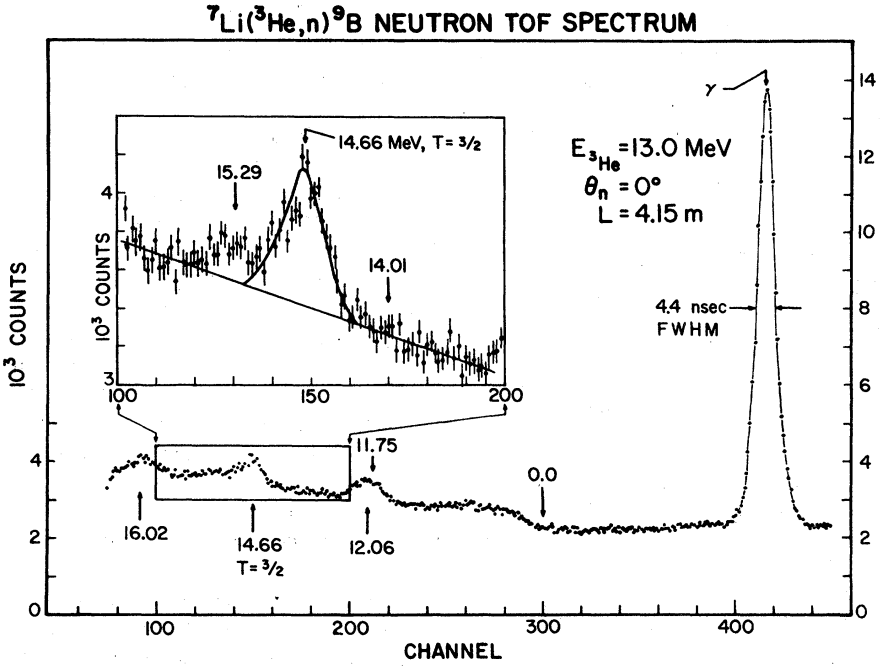

FIG. 7. Neutron TOF spectrum from ^{7}Li(^{3}He, n)^{9}B with a pulsed ^{3}He beam used to determine the yield of the $T=\frac{3}{2}$ state in singles. TAC start is provided by the neutron detector; stop by the tandem buncher system. Insert shows region around $T=\frac{3}{2}$ state enlarged. Straight line is the linear background subtracted to obtain peak yield.

rections are included, the error in the normalized singles yield is ±5.0%.

C. NaI efficiency and line shape

The response function or line shape of the NaI spectrometer for monoenergetic γ rays was obtained at 15.11 and 11.615 MeV, energies which bracket the prominent γ_0 and γ_2 peaks in each of the $T=\frac{3}{2}$ decay spectra. At 15.11 MeV the absolute efficiency was measured just prior to the ^{9}Be data runs using the same (^{3}He, $p\gamma$) coincidence setup. The 15.11 MeV 1^+, $T=1$ level of ^{12}C was excited via the ^{10}B(^{3}He, p) reaction at 4.1 MeV. A self-supporting 60 μg/cm^2 enriched ^{10}B target was bombarded with a 500 nA beam of ^{3}He$^+$ and protons were detected at 0°. Since the p-γ angular correlation is of the form $A_0+P_2P_2(\cos\theta)$ for both $J=1$ and $J=\frac{3}{2}$ levels, the γ rays were again detected at 125°.

Proton singles and coincidence spectra at 0° are shown in Fig. 8. The coincidence peak shape was used to fit the singles spectrum as in the ^{9}Be experiment, but a second peak was added to account for the ^{12}C(^{3}He, p_0)^{14}N contaminant group nearby. The statistical uncertainty in the singles peak area resulting from the fit was ±4.5%.

The 15.11 MeV γ-ray spectrum is shown in the upper part of Fig. 9. The line shape was extra-

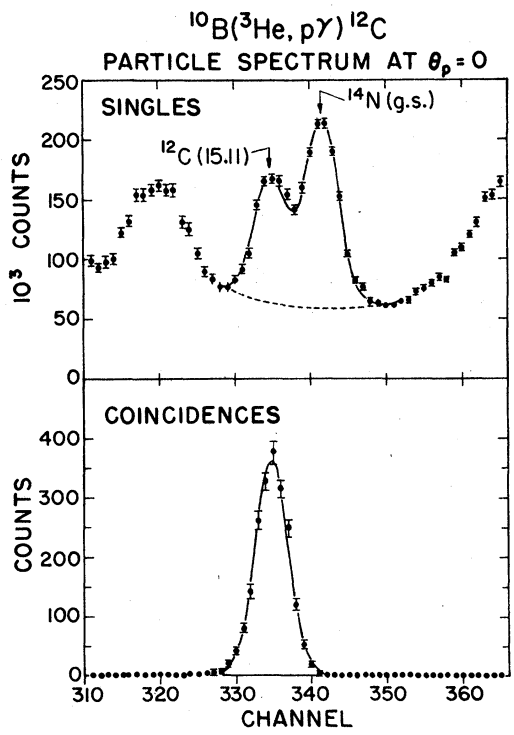

FIG. 8. Particle singles and coincidence spectra at 0° from the ^{10}B(^{3}He, $p\gamma$)^{12}C reaction used to measure the NaI efficiency at 15.11 MeV. Solid curves are as in Fig. 3.

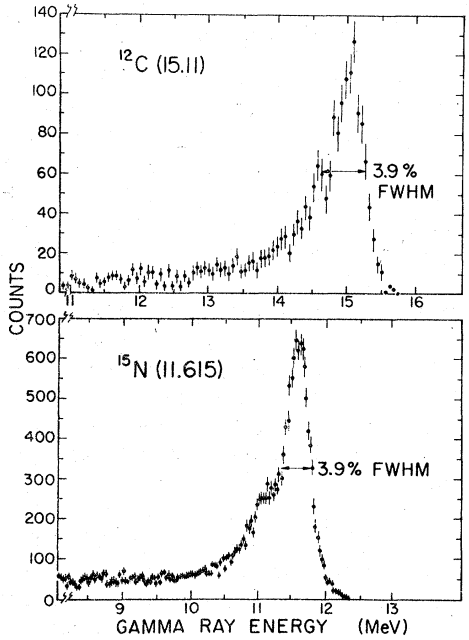

FIG. 9. High energy portions of monoenergetic γ-ray spectra in the NaI detector. These spectra were used to provide line shapes for fitting the mass 9 $T=\frac{3}{2}$ decay spectra. Upper spectrum from ^{10}B(^{3}He, $p\gamma$)^{12}C was also used to determine the NaI absolute efficiency. Lower spectrum is from ^{14}C(p,γ)^{15}N.

polated horizontally to zero energy from 11 MeV; however the fitting procedure used to extract the branching ratios does not depend on the tail region of the line shape. Using the known[2] (88.2 ± 2.1)% ground state branching ratio for ^{12}C(15.11), we obtained a total efficiency of $\epsilon\Omega/4\pi = (4.92 \pm 0.28) \times 10^{-3}$. This value is consistent with the more precise result $(4.63 \pm 0.17) \times 10^{-3}$ measured[12] in the mass 13 γ-decay experiment which employed the same γ detector and geometry. We used the weighted average of the two values, $(\epsilon\Omega/4\pi)$ (15.11 MeV) $= (4.75 \pm 0.16) \times 10^{-3}$. The efficiency was interpolated to energies between 11 and 15 MeV using γ-ray absorption coefficients. We note that comparisons of *relative* γ-ray branching ratios in the mirror nuclei are free from errors in the NaI efficiency because the mirror transitions have nearly the same energies.

A second response function was obtained for 11.615 MeV γ rays with the reaction ^{14}C(p,γ)^{15}N at $Ep = 1.51$ MeV, populating the lowest $T=\frac{3}{2}$ state of ^{15}N at 11.615 MeV. The high lying (5.27 MeV) first excited state of ^{15}N ensures a clean γ_0 spectrum. Care was taken to reproduce the same electronic efficiency (as evidenced by the accept/reject ratio) as was used in the decay experiments. As seen in Fig. 9 the energy resolution at 11.6 MeV remains 3.9%, but at this energy a first escape shoulder is evident.

The NaI response at intermediate energies was calculated by a computer code which interpolated between the two measured spectra, maintaining the correct photopeak to first escape peak spacing. Line shapes used to fit decays to states with finite natural widths required folding the interpolated response function with a Breit-Wigner resonance form weighted by E_γ^3. The fitting routine adjusted only the height of the line shape to fit the data, keeping the transition energy fixed.

III. RESULTS

A. γ-ray branching ratios

Least squares fits were made to the γ-ray spectra to determine the branching ratios of the $T=\frac{3}{2}$ levels. The best fits are shown as solid curves in Fig. 4. (The dashed curves indicate the contributions of the individual γ rays.) The quality of the fits is excellent except in the region near 3 MeV excitation in ^{9}Be, where the data exhibit a sharper peak than we could reproduce in any fits. Since the 3 MeV region falls near the first escape peak of the 11.97 MeV γ ray the deduced branching ratios to ^{9}Be(3.06) and ^{9}Be(2.8) are sensitive to the NaI line shape for γ rays of about 12 MeV. Our measurement of the line shape at 11.615 MeV is sufficiently near in energy to E_{γ_2} that the interpolation procedure should give an accurate response function at 11.97 MeV. In the fit shown in Fig. 4, transitions to both the 3.06 and 2.8 MeV states were allowed. The result for the branch to the broad 2.8 MeV state is consistent with zero. Only when the transition to ^{9}Be(3.06) was omitted did the fit ascribe any yield to ^{9}Be(2.8); however, the χ^2 was poorer with the 2.8 MeV state than with the sharper 3.06 MeV state. Our result is in disagreement with the observation by Adloff *et al.*[10] of a significant decay branch to the 2.8 MeV level $(\Gamma_\gamma(2.8)/\Gamma_\gamma(0) = 0.36)$. We therefore sought independent information on the ratio $\Gamma_{\gamma(3.06)}/\Gamma_{\gamma(2.8)}$ from an n-γ coincidence experiment. This measurement, described in detail in Sec. III B, also indicated that the γ-ray decay branch to the 2.8 MeV state is much smaller than that to the 3.06 MeV state.

The branching ratios to the known low-lying levels of ^{9}Be and ^{9}B deduced from the fitted γ-ray spectra are summarized in Table I and compared to those reported for ^{9}Be by Adloff *et al.*[10] The corresponding branching ratios in ^{9}B have not been previously measured. Our branching ratios Γ_{γ_0}/Γ and Γ_{γ_2}/Γ for the strong $M1$ decays in ^{9}Be are consistent with the previous results but have much smaller uncertainties. However, our data rule out the strong branch reported for the $\frac{1}{2}^-$

TABLE I. Summary of branching ratios of $T=\frac{3}{2}$ levels in ^{9}Be and ^{9}B.

	^{9}Be Γ_{γ_i}/Γ (%)		^{9}B
J of final state	This work	Adloff *et al.* Ref. 10	This work
$\frac{3}{2}^-$(g.s.)	1.81 ± 0.09	2.1 ± 0.4	1.85 ± 0.15
$\frac{1}{2}^+$	0.03 ± 0.04	···	0.00 ± 0.08
$\frac{5}{2}^-$	2.05 ± 0.11	2.5 ± 0.6	1.93 ± 0.22
$\frac{1}{2}^-$	<0.2	0.75 ± 0.17	0.31 ± 0.18
$\frac{5}{2}^+$	0.33 ± 0.07		
$\frac{3}{2}^+$	0.23 ± 0.05	···	···
$\Gamma_{\gamma_2}/\Gamma_{\gamma_0}(^9\text{Be}) = 1.13 \pm 0.05$		$\Gamma_{\gamma_2}/\Gamma_{\gamma_0}(^9\text{B}) = 1.03 \pm 0.11$	
$B_{\gamma_2}/B_{\gamma_0}(^9\text{Be}) = 1.97 \pm 0.12$		$B_{\gamma_2}/B_{\gamma_0}(^9\text{B}) = 1.74 \pm 0.19$	

state. As expected, the strong mirror $M1$ γ_0 and γ_2 decays display no charge asymmetry. Interpretation of the mirror decays to the $\frac{5}{2}^+$ states is difficult because the $\frac{5}{2}^+$ and $\frac{1}{2}^-$ levels have not been separately identified in ^{9}B. In our fits the branching ratios to the 2.78 MeV "state" in ^{9}B and the 3.06 MeV state in ^{9}Be are equal within errors.

Adloff *et al.*[10] deduced only the ground state branch Γ_{γ_0}/Γ from their coincidence γ-ray spectrum, obtaining the relative decay branches to the excited states from subsidiary measurements of $\Gamma_{\gamma(\text{excited})}/\Gamma_{\gamma_0}$. In the case of $\Gamma_{\gamma_2}/\Gamma_{\gamma_0}$, a Ge(Li) detector was placed at $\theta_\gamma = 0°$ rather than 125° and no correction was made for the p-γ angular correlation. Because they were unable to resolve the $\gamma(2.8)$ or $\gamma(3.06)$ transitions from $\gamma(2.43)$ in their NaI spectrum, Adloff *et al.* extracted the ratio $\Gamma_{\gamma(2.8)}/\Gamma_{\gamma(2.43)} = 0.30 \pm .04$ from the coincident neutron decay spectrum of the low-lying states assuming that the $\frac{1}{2}^-$ level decays 100% of the time to ^{8}Be(g.s.), although the neutron decay branching ratio is poorly known and could be as small as 50%.[13] They estimated 1.3 as an upper limit for $\Gamma_{\gamma(3.06)}/\Gamma_{\gamma(2.8)}$, but assumed $\Gamma_{\gamma(3.06)} = 0$, a result inconsistent with our higher resolution γ-ray spectrum.

We had hoped to observe the weak $E1$ decays to the $\frac{1}{2}^+$ first excited states of ^{9}Be and ^{9}B. The analogous $E1$ decays in ^{13}C and ^{13}N show a considerable asymmetry,[2] which is too large to be accounted for by isospin mixing or binding energy differences and has been attributed to charge dependent configuration mixing. Unfortunately the $\frac{1}{2}^+$ levels in mass 9 are quite broad, and our statistical uncertainties are too great to allow any meaningful comparison of transitions to these levels.

B. n-γ coincidences in ^{9}Be

The difficulty we experienced in fitting our ^{9}Be γ-ray spectrum near 3 MeV excitation and the small deduced branch to ^{9}Be(2.8), which disagrees with the value found by Adloff *et al.*, led us to look at decay neutrons from the low-lying states of ^{9}Be in coincidence with the γ rays from the $T=\frac{3}{2}$ level which feed these levels. Since the 2.43 MeV state breaks up 84% of the time into the three-body $\alpha+\alpha+n$ channel,[13] whereas both the 3.06 and 2.8 MeV states decay predominantly to ^{8}Be(g.s.) via the emission of higher energy neutrons,[11,13] the neutron energy can be used to discriminate against the three-body decays and thereby greatly reduce the 2.43 MeV state yield in the coincident γ-ray spectrum.

Our n-γ runs were made just above the threshold for populating the $T=\frac{3}{2}$ level in ^{9}Be ($E_{^3\text{He}} = 5.5$ MeV), in order to minimize the neutron energy spread arising from the ^{9}Be recoils. This bombarding energy is below the threshold for ^{7}Li(^{3}He, n)^{9}B(14.67), so γ decays in ^{9}B do not occur. The γ rays were detected with the NaI detector at $\theta_\gamma = 90°$ to maximize the detector solid angle and neutrons were detected at 30° over a 65 cm flight path. Without a measurement of the n-γ angular correlation this geometry precludes a rigorous determination of branching ratios, but gives a good qualitative measure of the strength of the branches. Neutron TOF spectra in coincidence with γ rays in three different energy windows are shown in Fig. 10. The arrows point to the expected positions of neutrons from the indicated states in ^{9}Be decaying via ^{8}Be(g.s.)+n. In each case the solid curve shows the random background plus the expected three-body decay spectrum for

$$^9\text{Be}(2.43) \rightarrow {}^5\text{He} + \alpha \searrow \alpha + n$$

assuming all decays are isotropic in their center of mass. The energy dependence of the neutron detector efficiency has been neglected; this accounts for the overestimation of the yield at low neutron energies. The γ-ray window for the middle spectrum excludes essentially all but the decays of the 2.43 MeV state. In the lower spectrum, however, a narrow peak due to decays of the 3.06 MeV, $\frac{5}{2}^+$ state is evident. Decay neutrons from the 2.8 MeV state would be more difficult to observe because of the greater width of the state and its possible (up to 40%) decay mode into $\alpha+\alpha+n$.

Spectra of γ rays in coincidence with neutrons in regions I and II of the TOF spectrum are shown in

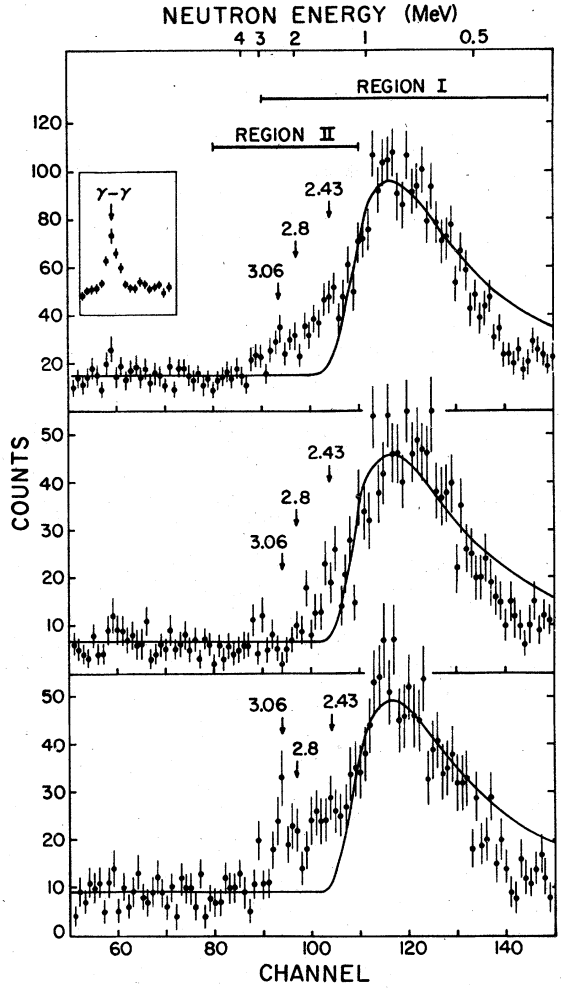

FIG. 10. Neutron TOF spectra from decays of low-lying ^{9}Be levels excited via ^{7}Li(^{3}He,$p\gamma$)^{9}Be for three different γ-ray energy windows; 10.8 MeV $\leq E_\gamma \leq$ 12.6 MeV (upper), 11.6 MeV $\leq E_\gamma \leq$ 12.6 MeV (middle), and 10.8 MeV $\leq E_\gamma \leq$ 11.6 MeV (lower). Arrows show expected locations of peaks from decays to ^{8}Be(g.s.). Solid curve shows random background plus contribution from ^{9}Be (2.43) $\rightarrow 2\alpha + n$ calculated as described in the text neglecting neutron detector efficiency. Inset shows a sort with a window on low energy γ rays to indicate the position of the prompt γ-γ coincidence peak.

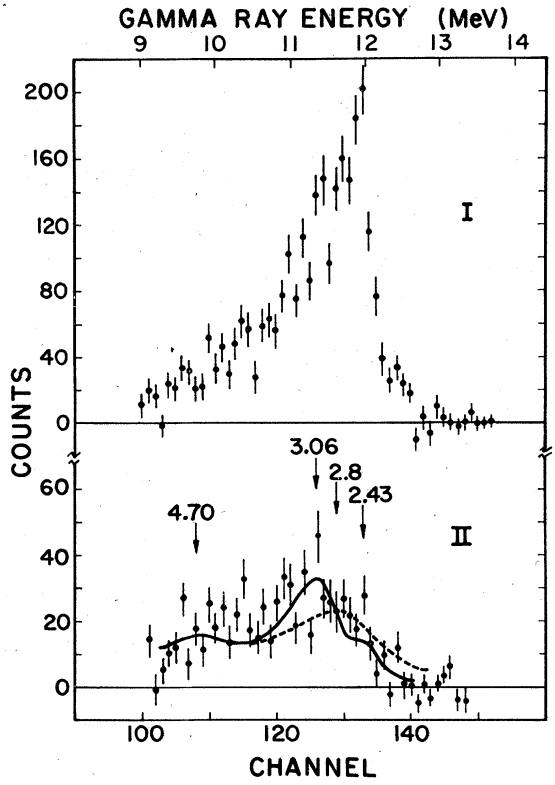

FIG. 11. Spectra of γ rays from decays of $T = \frac{3}{2}$ level in ^{9}Be in coincidence with decay neutrons in regions I and II of the TOF spectra of Fig. 10. Solid curve is least squares fit including decays to excited states of ^{9}Be at 4.7, 3.06, 2.8, and 2.43 MeV. Dashed curve is fit in which 3.06 MeV state is excluded.

Fig. 11. The upper spectrum (region I) is dominated by decays to ^{9}Be(2.43). The lower γ ray spectrum corresponds to region II, which encompasses the n_0 decays of all the low-lying states of ^{9}Be. The contribution of 11.97 MeV γ rays to this spectrum is quite small. We have made least squares fits to this spectrum to extract the yields of the various γ rays. The solid curve is a fit in which the 4.7, 3.06, 2.8, and 2.43 MeV states were included. The dashed curve, in which the 3.06 MeV state was excluded, is clearly a much poorer fit to the data than the solid curve. The solid curve gives the following yields for the 3.06 and 2.8 MeV states: $Y(3.06) = 460$ counts ±12%, $Y(2.8) = 129$ counts ±79%. Neglecting the n-γ angular correlations, the center of mass to lab transformations, and the neutron detector efficiency (these latter two corrections are very small for the two n_0 decays), the n-γ yields would imply that

$$\Gamma_{\gamma(2.8)}/\Gamma_{\gamma(3.06)} = 0.24^{+0.26}_{-0.19} \quad \text{if} \quad \frac{\Gamma_{n_0}}{\Gamma}\bigg|_{2.8} = 100\%,$$

or

$$\Gamma_{\gamma(2.8)}/\Gamma_{\gamma(3.06)} = 0.40^{+0.43}_{-0.33} \quad \text{if} \quad \frac{\Gamma_{n_0}}{\Gamma}\bigg|_{2.8} = 60\%.$$

These results are consistent with our conclusion, based on the ^{7}Li(^{3}He,$p\gamma$) γ-ray spectrum, that the branch to ^{9}Be(2.8) is small. The branching ratios we report are taken from the (^{3}He,$p\gamma$) data and not from the n-γ coincidence measurement which was performed in a complicated correlation geometry.

TABLE II. γ transition strengths from the lowest ($\frac{3}{2}^-$, $T=\frac{3}{2}$) state in ^{9}Be and β-decay strengths from ^{9}Li.

Final state E_f (MeV)	J^π	Γ_γ (eV)	Measured γ-decay strengths Present results [a] $B_{W.u.}$	Λ_γ ($M1$) [b]	Previous work [c] Λ_γ ($M1$) [b]	Calculated Λ_γ ($M1$) Barker [d]	Barker [e]	CK [f]	β transition strengths Λ_β for ^{9}Li Experiment [g]	Theory Barker [d]	Barker [e]
0	$\frac{1}{2}^-$	6.9±0.5	0.11±0.01	0.84±0.06	0.85±0.16	0.62	0.52	1.31	0.25	0.17	0.11
2.43	$\frac{5}{2}^-$	7.8±0.7	0.22±0.02	1.65±0.15	1.7	1.05	1.88	1.20	0.33	0.17	0.52
2.8	$\frac{1}{2}^-$	<0.8	<0.02	<0.2	0.60	0.10	0.07	0.50	0.035	0.15	0.08
3.06	$\frac{5}{2}^+$	1.2±0.3	(2.9 ±0.7)×10^{-3}								
4.7	$\frac{3}{2}^+$	0.9±0.2	(3.4 ±0.8)×10^{-3}								

[a] Based on $\Gamma_{\gamma_0}=6.9\pm0.5$ eV (Ref. 14).
[b] Assuming $\Gamma_\gamma(E2)\ll\Gamma_\gamma(M1)$.
[c] Reference 10, normalized as above.
[d] Reference 15, using interaction of Ref. 16.
[e] Reference 15, using interaction of Ref. 17.
[f] Cohen and Kurath (from Ref. 10).
[g] Reference 13.

IV. DISCUSSION

A. γ-ray transition strengths in ^{9}Be

The ground state radiative width of Γ_{γ_0} of the lowest $T=\frac{3}{2}$ state in ^{9}Be has been measured by inelastic electron scattering[14] with the result $\Gamma_{\gamma_0}=6.9\pm0.5$ eV. Combining this value with our measured branching ratios from Table I we obtain the partial widths for γ decay to excited states of ^{9}Be, given in Table II, column 3. In column 4, the reduced transition strengths $B_{W.u.}$ in Weisskopf units are given for all observed transitions. For the $M1$ transitions we show in column 5 the reduced transition strength $\Lambda_\gamma(M1)$ calculated from the expression $\Lambda_\gamma(M1)=362\ \Gamma_\gamma(\mathrm{eV})/E_\gamma^3(\mathrm{MeV})$. Theoretical predictions for $\Lambda_\gamma(M1)$ are listed in columns 7–9 for comparison to our experimental results. Barker[15] has calculated the $M1$ γ ray transition strengths using his own interaction[16] and also using an interaction more recently given by Kumar.[17] The results of Cohen and Kurath (CK) are taken from the paper by Adloff *et al.*[10]

Barker's calculation with his own interaction comes closest to predicting both the ground state γ decay strength Λ_{γ_0} and the ratio $\Lambda_{\gamma_2}/\Lambda_{\gamma_0}$ for the two strongest transitions, although his result is somewhat outside the experimental errors. His predicted strength for the transition to the $\frac{1}{2}^-$ level at 2.8 MeV is an order of magnitude weaker than that to the $\frac{5}{2}^-$, in agreement with the present experimental result, whereas the calculation by Cohen and Kurath predicts a much larger value for the transition strength to $\frac{1}{2}^-$(2.8 MeV).

The β decay of ^{9}Li also populates the low-lying negative parity levels of ^{9}Be. The measured[13] and calculated[16] analogous β decay strengths are expressed as $\Lambda_\beta=7.4\times4390/ft$ (Ref. 18) (appropriate for $T=\frac{3}{2}\rightarrow T=\frac{1}{2}$) and are listed in Table II. These strengths represent the spin contribution to the $M1$ γ decays feeding the same levels. Hanna[18] and Dietrich[19] have stressed the importance of the orbital contribution to $M1$ γ decay strengths in this mass region, and in the case of γ_0 and γ_2 both the experimental and theoretical γ decay strengths are in fact much larger than the corresponding β decay strengths, as is the case for the analog to antianalog decay[19] of ^{13}N($\frac{3}{2}^-$, $T=\frac{3}{2}$). On the other hand, for the transition to $\frac{1}{2}^-$(2.8 MeV), three calculations by Barker[15] using interactions of Barker,[16] Kumar,[17] and Cohen and Kurath[20] all show that $\Lambda_\gamma\approx\Lambda_\beta$. Since the experimental β decay strength to $\frac{1}{2}^-$(2.8 MeV) is very weak[13] [$\Lambda_\beta(\frac{1}{2}^-)=.035$], it seems reasonable that the corresponding γ-ray decay would also be weak. Our results indicate that this is indeed the case.

Let us now discuss the $E1$ transitions. We have observed branches to the $\frac{5}{2}^+$, 3.06 MeV and $\frac{3}{2}^+$,

TABLE III. Two level isospin mixing.

^{9}Be				^{9}B			
$E(T=\frac{1}{2})$	$\Gamma(T=\frac{1}{2})$	α^2 (%)	$\langle H_{CD}\rangle$ (keV)	$E(T=\frac{1}{2})$	$\Gamma(T=\frac{1}{2})$	α^2 (%)	$\langle H_{CD}\rangle$ (keV)
11.28	575	0.07	80	11.75	800	0.05	63
11.81	400	0.1	80	12.06	800	0.05	50
13.79	590	0.06	15	14.01	390	0.09	20
Theory [a] Coulomb only							
12.76		0.01	17.3	12.76		0.001	−4.7

[a] Reference 23.

4.70 MeV states. The shell model calculations discussed above do not include s-d shell excitations and therefore make no predictions regarding positive parity states. The simplest model for the positive parity ($\frac{1}{2}^+$, $\frac{3}{2}^+$, and $\frac{5}{2}^+$) states (weak coupling of $2s$ or $1d$ neutrons to the 0^+ or 2^+ states of ^{8}Be) would predict zero transition strength from the $T=\frac{3}{2}$ level, which is a 2p-1h p shell excitation.[15,16] While we do not observe transitions to the $\frac{1}{2}^+$ level (at 1.67 MeV) we do find weak branches of nearly equal reduced strength to the $\frac{3}{2}^+$ and $\frac{5}{2}^+$ levels. (See Table II.) These have strengths comparable to similar $E1$ decays of the lowest $\frac{3}{2}^-$ $T=\frac{3}{2}$ levels in mass 13 for which[2] $B(E1)\sim 5\times 10^{-3}$ W.u. In ^{9}Be as well as mass 13 a comparison of $E1$ strengths indicates that these γ decays should not be strongly affected by isospin mixing.

B. Comparison of isospin mirror γ decays; isotensor electromagnetic interaction

Since the ground state γ decay width of the 14.66 MeV $T=\frac{3}{2}$ state in ^{9}B is not known, we cannot compare reduced transition probabilities for individual mirror decays in ^{9}Be and ^{9}B. The ratio of the reduced strengths $B_{\gamma_2}/B_{\gamma_0}$, which is independent of the absolute strengths, gives the most precise comparison of the $\Delta T=1$, $M1$ transitions. Following Ref. 2 we define the asymmetry parameter

$$\Delta \equiv \frac{B_{\gamma_2}(^9\mathrm{Be})}{B_{\gamma_0}(^9\mathrm{Be})}\,\frac{B_{\gamma_0}(^9\mathrm{B})}{B_{\gamma_2}(^9\mathrm{B})} - 1 .$$

Substituting our measured values of $B_{\gamma_2}/B_{\gamma_0}=1.97\pm0.12$ for ^{9}Be and 1.76 ± 0.21 for ^{9}B gives $\Delta=0.12\pm0.13$, in agreement with the selection rule for mirror isovector γ transitions. Since the $M1$ transitions are relatively insensitive to fine details of nuclear structure, we can derive an upper limit for the isotensor electromagnetic transition amplitude from the uncertainty in the measurement of the asymmetry. If A_2 and A_1 denote the reduced isotensor and isovector transition amplitudes, respectively, then the asymmetry expected in the ratio of $M1$ transitions is

$$\Delta = 8(\tfrac{3}{5})^{1/2}\overline{A} ,$$

where

$$\overline{A} \equiv \frac{1}{2}\left(\frac{A_2(\gamma_2)}{A_1(\gamma_2)} - \frac{A_2(\gamma_0)}{A_1(\gamma_0)}\right) .$$

The experimental result implies $\overline{A}=(1.9\pm2.1)\%$, or an upper limit of 4.1%. This is less restrictive than the 1.6% upper limit found in mass 13 but is the only such measurement for mass 9. In the unlucky event that A_2 and A_1 have equal magnitudes and phases for the γ_0 and γ_2 transitions, the upper limit on $\overline{A}$ would not restrict A_2/A_1. For that reason, measurements in a variety of nuclei are useful, and our upper limit for $\overline{A}$ gains significance when coupled with the similar result in mass 13.

Theoretical calculations of the expected asymmetry in isovector $M1$ decays resulting from a hypothetical isotensor current have been carried out for mass 9 and mass 13 by Chemtob and Furui.[4] Their results are much smaller than the experimental upper limits in both cases: $\Delta=-0.7\%$ in mass 13 and −0.5% in mass 9.

C. Total widths of $T=3/2$ levels; isospin mixing in mass 9

The total width of the lowest $T=\frac{3}{2}$ level in ^{9}Be, $\Gamma(^9\mathrm{Be})=381\pm33$ eV, can be obtained by combining our value of Γ_{γ_0}/Γ with the value[14] Γ_{γ_0} 6.9 ± 0.5 eV obtained from inelastic electron scattering. The total width of the corresponding level in ^{9}B cannot be obtained directly. This is ordinarily done by combining resonance strength and branching ratio measurements. In this case the required targets are not stable. The width in ^{9}B must be inferred indirectly under the assumption that $B_{\gamma_0}(^9\mathrm{B}) = B_{\gamma_0}(^9\mathrm{Be})$. This equality of mirror $\Delta T=1$ γ-ray transitions is, of course, expected if the electromagnetic interaction is isoscalar plus isovector and if isospin mixing effects can be neglected. We

expect that isospin mixing will have only a small effect on the strong $M1$ γ_0 transitions in mass 9. This is consistent with our measured Δ which is zero within errors and with the relatively precise measurements of the γ_0 decays of the lowest $T=\frac{3}{2}$ levels in mass 13 which give $B_{\gamma_0}(^{13}\mathrm{N})/B_{\gamma_0}(^{13}\mathrm{C})$.

Assuming that $B_{\gamma_0}(^9\mathrm{B})=B_{\gamma_0}(^9\mathrm{Be})$ and using our measured absolute γ_0 branching ratios in ^{9}Be and ^{9}B we obtain $\Gamma(^9\mathrm{B})=395\pm42$ eV where the errors reflect only the uncertainties in the experimental quantities. The errors in $\Gamma_{\gamma_0}(^9\mathrm{Be})$ and in the NaI efficiency cancel when computing the ratio of total widths, so we obtain with higher precision $\Gamma(^9\mathrm{B})/\Gamma(^9\mathrm{Be})=1.04\pm0.10$. These results are consistent with the less precise values $\Gamma(^9\mathrm{Be})=329\pm67$ eV, $\Gamma(^9\mathrm{B})=275\pm93$, and $\Gamma(^9\mathrm{B})/\Gamma(^9\mathrm{Be})=0.84\pm0.33$ deduced from previous work.[9] If we allow for a generous ±10% uncertainty in the Γ_{γ_0} values, the error in the ratio of total widths would be ±0.14, still considerably less than the previous error.

This equality of total widths in mass 9 is a strong exception to all other known decays of $T=\frac{3}{2}$ levels, which range from mass 13 to mass 25, and for which the ratio $\Gamma(T_z=\frac{1}{2})/\Gamma(T_z=-\frac{1}{2})$ lies between 4 and 12. Since the neutron channel is barely open in mass 25 one must compare reduced widths in this case; in all other cases these comparisons are not altered significantly by using reduced widths, since the somewhat greater energy available for proton decay is roughly compensated by the increased (Coulomb) barrier. This equality is also contrary to recent schematic model predictions[21] that in mass 9, as in heavier systems, the $T=\frac{3}{2}$, $T_z=\frac{1}{2}$ level should be broader than the $T=\frac{3}{2}$, $T_z=-\frac{1}{2}$ level. Theoretical calculations[22,23] of Coulomb mixing specific to mass 9 are inconsistent on this issue, and disagree also with the magnitudes of the total widths. The experimental magnitudes are empirically consistent with $\langle H_{\mathrm{CD}}\rangle\sim20$–$80$ keV if the mixing is dominated by nearby $T=\frac{1}{2}$ levels. This is illustrated in Table III where values of α^2 and $\langle H_{\mathrm{CD}}\rangle$ are shown for several possible candidates for the admixed $T=\frac{1}{2}$ level (assuming single level mixing). These $\langle H_{\mathrm{CD}}\rangle$ values are not uncommonly large compared to other known examples in light nuclei.

V. CONCLUSION

We have made the most precise measurement to date of the γ-ray branching ratios of the lowest $T=\frac{3}{2}$ analog states in ^{9}Be and ^{9}B and have found no violation of the selection rule for $\Delta T=1$ mirror γ-ray transitions. No evidence for isotensor electromagnetic currents is seen, but our 4% upper limit for A_2/A_1 is still far above theoretical expectations. We find the γ-ray branch to the $\frac{1}{2}^-$, 2.8 MeV state in ^{9}Be to be much smaller than reported previously,[10] but not in serious disagreement with the analogous branch from ^{9}Li β decay.[13] A significant branch to the $\frac{5}{2}^+$, 3.06 MeV state, discounted in earlier work,[10] is now shown to be larger than the branch to ^{9}Be(2.8).

The total widths of the $T=\frac{3}{2}$ levels have been deduced from the branching ratios assuming equal reduced ground state radiative widths for the mirror levels. These total widths are equal to each other within 10% uncertainty and constitute a strong exception to the trend for $\Gamma(T_z=\frac{1}{2})\gg\Gamma(T_z=-\frac{1}{2})$ established for other $4N+1$ nuclei.[2,5-8] Interpretation of these widths as evidence of specific isospin impurities is hindered by incomplete knowledge of the spins, parities, widths, and decay properties of the $T=\frac{1}{2}$ levels.

---

*Present address: Cyclotron Laboratory, Michigan State University, East Lansing, Michigan 48824.

†Research supported by the U.S. Energy Research and Development Agency.

[1]E. K. Warburton and J. Wesener, in *Isospin in Nuclear Physics*, edited by D. H. Wilkinson (North-Holland, Amsterdam, 1969), p. 173.

[2]R. E. Marrs, E. G. Adelberger, and K. A. Snover, Phys. Rev. C 16, 61 (1977).

[3]R. J. Blin-Stoyle, Phys. Rev. Lett. 23, 535 (1969).

[4]M. Chemtob and S. Furui, Nucl. Phys. A233, 435 (1974).

[5]A. B. McDonald, T. K. Alexander, and O. Häusser, Nucl. Phys. A273, 464 (1976).

[6]A. B. McDonald, H. B. Mak, H. C. Evans, G. T. Ewan, and H. B. Trautvetter, Nucl. Phys. A273, 477 (1976).

[7]H. Weigmann, R. L. Macklin, and J. A. Harvey, Phys. Rev. C 14, 1328 (1976).

[8]P. G. Ikossi, W. J. Thompson, T. B. Clegg, W. W. Jacobs, and E. J. Ludwig, Phys. Rev. Lett. 36, 1357 (1976).

[9]A. B. McDonald, T. K. Alexander, O. Häusser, D. Disdier, E. G. Adelberger, H. B. Mak, A. P. Shukla, and A. V. Nero, Nucl. Phys. A273, 451 (1976).

[10]J. C. Adloff, K. H. Souw, and C. L. Cocke, Phys. Rev. C 3, 1808 (1971).

[11]P. R. Christensen and C. L. Cocke, Nucl. Phys. 89, 656 (1966).

[12]R. E. Marrs, Ph.D. thesis, University of Washington, 1975 (unpublished).

[13]Y. S. Chen, T. A. Tombrello, and R. W. Kavanagh, Nucl. Phys. A146, 136 (1970).

[14]J. C. Bergstrom, I. P. Auer, M. Ahmed, F. J. Kline, J. H. Hough, H. S. Caplan, and J. L. Groh, Phys. Rev. C 7, 2228 (1973).

[15]F. C. Barker, private communication.

[16]F. C. Barker, Nucl. Phys. 83, 418 (1966).

[17]N. Kumar, Nucl. Phys. A225, 221 (1974).

[18]S. S. Hanna, in *Isospin in Nuclear Physics* (see Ref. 1),

p. 1.
[19]F. S. Dietrich, M. Suffert, A. V. Nero, and S. S. Hanna, Phys. Rev. 168, 1169 (1968).
[20]S. Cohen and D. Kurath, Nucl. Phys. 73, 1 (1965).
[21]A. B. McDonald and E. G. Adelberger, Phys. Rev. Lett. 40, 1692 (1978).
[22]M. Tomaselli, Z. Phys. 233, 240 (1970).
[23]W. K. Lin, Phys. Lett. 34B, 480 (1971).